

PRINCIPAL FOLIATIONS OF SURFACES NEAR ELLIPSOIDS

JOHN GUCKENHEIMER

To Vaughan Jones

(Received 6 June, 2021)

Abstract. The lines of curvature of a surface embedded in \mathbb{R}^3 comprise its principal foliations. Principal foliations of surfaces embedded in \mathbb{R}^3 resemble phase portraits of two dimensional vector fields, but there are significant differences in their geometry because principal foliations are not orientable. The Poincaré-Bendixson Theorem precludes flows on the two sphere S^2 with recurrent trajectories larger than a periodic orbit, but there are convex surfaces whose principal foliations are closely related to non-vanishing vector fields on the torus T^2 . This paper investigates families of such surfaces that have dense lines of curvature at a Cantor set C of parameters. It introduces discrete one dimensional return maps of a cross-section whose trajectories are the intersections of a line of curvature with the cross-section. The main result proved here is that the return map of a generic surface has *breaks*; i.e., jump discontinuities of its derivative. Khanin and Vul discovered a qualitative difference between one parameter families of smooth diffeomorphisms of the circle and those with breaks: smooth families have positive Lebesgue measure sets of parameters with irrational rotation number and dense trajectories while families of diffeomorphisms with a single break do not. This paper discusses whether Lebesgue almost all parameters yield closed lines of curvature in families of embedded surfaces.

1. Introduction

Vaughan Jones' generous support of the New Zealand Mathematics Research Institute, specifically the 2016 Raglan Summer School on Continuation Methods in Dynamical Systems, helped launch the work described here. Like Jones own work, this paper forges connections between different areas of mathematics – in this case differential geometry and dynamical systems. The primary objects of interest are principal foliations consisting of the lines of curvature on surfaces embedded in three space. They are similar to the phase portraits of dynamical systems, but differ in that their tangent line fields are not orientable like vector fields. Numerical methods for computing phase portraits of dynamical systems are a prominent part of dynamical systems theory, and they were the focus of the Raglan Summer School. While software that draws phase portraits of two dimensional vector fields is widely available, that has not been the case for principal foliations. Few examples of principal foliations appear in the mathematics literature, with the notable exception of surfaces of revolution and the foliations of triaxial ellipsoids. Baffled by the paucity of examples, I set out to create algorithms that visualize principal foliations, similar to those that draw phase portraits of vector fields. My journey has led me to

2010 *Mathematics Subject Classification* 53A05, 37C20, 37E45.

Key words and phrases: surface; line of curvature; return map.

a far richer world than I expected to find. In the spirit of Vaughan Jones, this paper is a travelogue, presenting an informal description of my recent discoveries. The interplay between algorithm development, careful study of numerical examples and mathematical theory that has been so illuminating in dynamical systems theory has again been indispensable in these investigations.

Dynamical systems theory studies the geometry of phase portraits of *generic* vector fields on compact manifolds. A seminal result is Peixoto's Theorem [14] characterizing structurally stable vector fields on orientable, compact two dimensional manifolds. Structurally stable vector fields on surfaces are characterized by the following four properties: (1) equilibrium points are hyperbolic, (2) periodic orbits are hyperbolic, (3) there are no saddle connections (trajectories that tend to saddles as $t \rightarrow \pm\infty$) and (4) all trajectories tend to an equilibrium point or closed curve as $t \rightarrow \pm\infty$. Moreover, vector fields satisfying these properties are dense in the space of C^r vector fields. Using these results as a backdrop, Sotomayor and Gutiérrez [16, 17], proved analogous results for principal foliations. The Poincaré-Bendixson Theorem [8] states that the fourth condition is satisfied by all vector fields on the two sphere S^2 , so is not needed in that case.

The simplest dynamical systems with large limit sets are non-vanishing vector fields on the two torus T^2 with a global cross-section Σ . Their return maps $\sigma : \Sigma \rightarrow \Sigma$ are smooth diffeomorphisms of the circle. The *rotation number* ρ is a continuous function on the space of circle diffeomorphisms that distinguishes the two types of dynamics that are possible: limit sets of diffeomorphisms with rational ρ are periodic orbits, while diffeomorphisms with irrational ρ have dense, quasiperiodic trajectories. In families of diffeomorphisms, quasiperiodic trajectories typically occur for positive measure sets of parameters. Principal foliations on surfaces close to triaxial ellipsoids are more similar to these vector fields on the torus than to dynamical systems on the sphere. I pursued that relationship in a previous paper [6] by lifting the non-orientable line field of principal foliations to vector fields on a double cover ramified at umbilic points. I gave one example in which the lifted vector field on the torus was rescaled to remove its equilibrium points, but that example now seems to be special. Here, I take a different approach to studying these principal foliations, constructing return maps to cross-sections of the foliations whose trajectories lie in the intersections of the cross-section with lines of curvature. In contrast to the return maps of dynamical systems, these return maps are *homeomorphisms* of the circle that are smooth except for *breaks* (jump discontinuities of their derivative) located at lines of curvature that approach an umbilic point without returning to the cross-section. Khanin and Vul [10] analyzed the dynamics of circle diffeomorphisms with a single break and found two qualitative differences with diffeomorphisms that have no breaks. First, diffeomorphisms with a single break do not have smooth invariant measures, and second, quasiperiodic dynamics occurs only for parameter sets of measure zero in generic families of diffeomorphisms with a single break. Khmelev [11] studied diffeomorphisms with multiple breaks, but did not fully answer questions about which families of such diffeomorphisms have quasiperiodic dynamics for positive measure sets of parameters.

In the rest of this paper, I recall the theory of generic vector fields on two manifolds and the parallel theory of principal foliations developed by Sotomayor

and Gutiérrez [16, 17]. Next, I describe how to produce circle homeomorphisms as return maps for principal foliations on simply connected surfaces with a minimal number of generic umbilic points. This is followed by a review of relevant aspects of the theory of circle diffeomorphisms and circle diffeomorphisms with breaks. Breaks in return maps of surfaces are the central issue examined in this paper. I present a numerical example and prove that return maps of generic principal foliations have breaks at separatrices that approach lemon umbilic points without returning to the cross-section. Finally, I apply the theory of circle diffeomorphisms with breaks to simply connected surfaces with only lemon umbilic points.

2. Principal Curvatures and Foliations

Let $S \subset \mathbb{R}^3$ be a smooth compact surface of genus 0; i.e., diffeomorphic to the two sphere S^2 . If $p \in S$, $N(p)$ is the unit (outward) normal to S at p , $\gamma(s)$ is a planar curve on S parameterized by arc length with $\gamma(0) = p$ and $\frac{d\gamma}{ds}(0) = v$, then the normal curvature at p in the direction v is $\kappa(p, v) = \frac{d^2(\gamma)}{ds^2}(0) \cdot N(p)$. If $\kappa(p, v)$ is not constant as a function of v , then its maximum and minimum values $\kappa_1 \geq \kappa_2$ are the *principal curvatures* at p . Points where the normal curvatures are constant in all directions are *umbilic points*. Elsewhere, vectors v_1 and v_2 whose normal curvatures are κ_1 and κ_2 are *principal vectors*. γ is a *line of curvature* if all of its tangent vectors lie in principal directions. *Rodrigues formula* states that the tangent vector $\frac{d\gamma}{dt}(p)$ to γ is a principal vector v if and only if $\frac{dN \circ \gamma}{dt}(p) = \kappa \frac{d\gamma}{dt}(p)$ [17]. In this case, κ is the principal curvature in the direction v . Rodrigues formula yields a system of equations whose solutions v are principal unit vectors [17]:

$$\begin{aligned} N \cdot v &= 0 \\ v \cdot v &= 1 \\ \det(N, v, dN \cdot v) &= 0 \end{aligned} \tag{2.1}$$

The equations (2.1) express that v is a tangent vector to S , v has unit length and that $dN \cdot v$ lies in the plane spanned by N and v . The first of these equations is linear in v while the second two are quadratic and even in v . Typically, there will be four solutions in two pairs of the form $\pm v$. If v_1 and v_2 are solutions that are not collinear, then they are orthogonal to each other since dN is a symmetric matrix.

Except at umbilic points, principal vectors v_1 and v_2 are distinguished from each other globally on S by the inequality $\kappa_1 > \kappa_2$; however, there is no way to choose the orientations of the principal vectors so that they vary continuously. As with equilibria of vector fields, the index of an umbilic point measures the number of rotations that the direction of the principal foliation makes when varied continuously along a closed curve surrounding the umbilic point. The index of a generic umbilic point is $\pm \frac{1}{2}$. Indeed, the orientation of a principal vector is reversed if it is continued around the boundary of a disk that encloses the umbilic point (and no others). Darboux [3] first classified generic umbilic points: there are three types, classified as lemons (one separatrix), monstars (two separatrices) and stars (three separatrices) [1]. Unlike trajectories of a vector field on S^2 , lines of curvature of an embedding of S^2 in R^3 can intersect a cross-section of the principal foliation with both orientations.

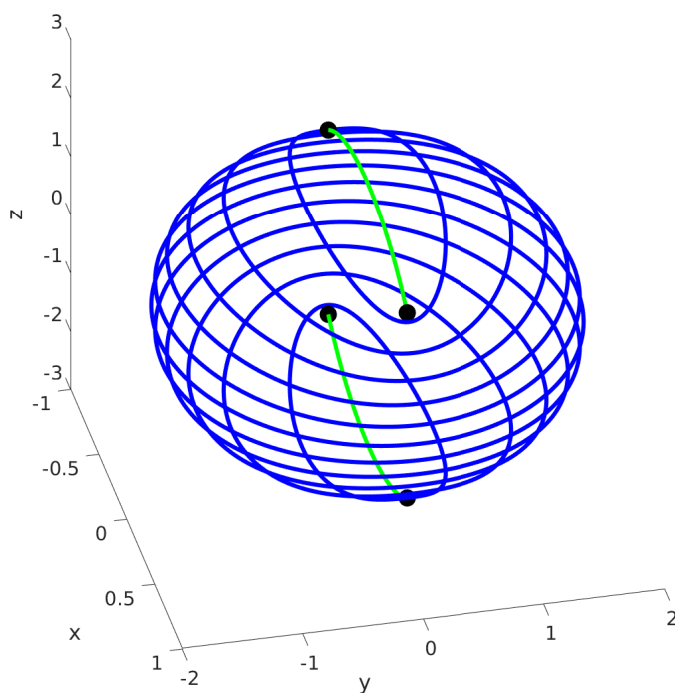


FIGURE 1. Maximal principal foliation on an ellipsoid. All of the lines of curvature are closed curves except two umbilic connections (plotted green). Umbilic points are large black dots. Note that the foliations is not orientable near an umbilic connection because a nearby line of curvature that follows the connection from front to back on its right makes a half turn around an umbilic at the end of the connection and follows it from back to front on the left side. More formally, if one traces the direction of the foliation continuously on a closed curve that surrounds an umbilic point, that direction rotates by π – returning with the opposite orientation.

Figure 1 displays a principal foliation of a triaxial ellipsoid S_0 . In 1796, Monge [13] found that the lines of curvature on the ellipsoid are intersections with hyperboloids in a triply orthogonal family of confocal quadric surfaces. There are four umbilic points, all lemons. Each principal foliation has two umbilic point separatrices, each connecting two of the umbilic points. All other lines of curvature on the ellipsoid are closed curves. Using this example as a starting point, I [6] investigated principal

foliations in the one parameter family of surfaces S_λ defined by

$$f_\lambda(x, y, z) = x^2 + \frac{1}{3}y^2 + \frac{1}{5}z^2 + \lambda xyz - 1, \quad |\lambda| < \lambda_0 \tag{2.2}$$

with $\lambda_0 > 0$ chosen so that the S_λ are all simply connected and have four umbilic points that are lemons. (See Garcia and Sotomayor [5], Exercise 3.6.3.) Throughout the remainder of this paper, I restrict attention to the class $\mathcal{S}_{\mathcal{L}}$ of simply connected surfaces S satisfying

- S has four umbilic points all lemons, and
- the maximal principal foliation of S is transverse to the coordinate plane $x = 0$.

Later, I restrict the class $\mathcal{S}_{\mathcal{L}}$ further.

Numerical computations of the principal foliations of S_λ discovered two types:

- (1) foliations with isolated lines of curvature, and
- (2) foliations with dense lines of curvature

Figure 2 shows both types. There are similarities between this family of principal foliations on S_λ and families of non-vanishing vector fields on the torus T^2 with a global cross-section. I [6] pursued this relationship by defining maps $T^2 \rightarrow S_\lambda$ that are double covers ramified at umbilic points and vector fields on T^2 that project to vectors in the principal foliations of S_λ in the complement of the umbilic points. Here I use an alternative approach to study the geometry of principal foliations of surfaces in $\mathcal{S}_{\mathcal{L}}$.

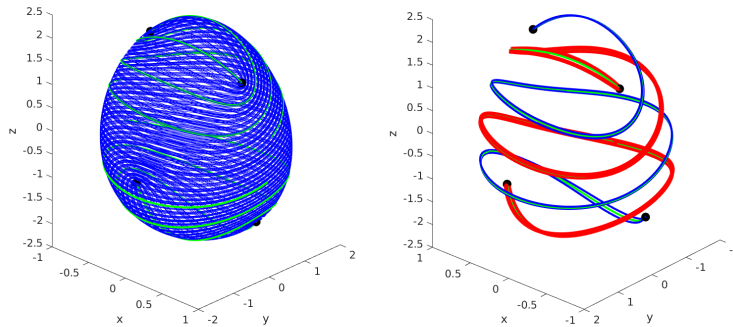


FIGURE 2. Maximal principal foliations on two surfaces in the family (2.2). Umbilic points are black dots and their separatrices are plotted green. On the left, the single blue trajectory of the surface $S_{0.11}$ appears to be dense. On the right, closed lines of curvature of $S_{0.1857}$ are plotted red and blue. All other lines of curvature tend to these closed ones.

The dynamics of some continuous time vector fields can be reduced to discrete time iterations by choosing cross-sections and defining their return maps. Parametrize the torus $T^2 = S^1 \times S^1$ with circular coordinates (θ_1, θ_2) . The circle Σ consisting of points with $\theta_1 = 0$ is a global cross-section Σ to vector fields with $\dot{\theta}_1 > 0$.

The return maps $\sigma : \Sigma \rightarrow \Sigma$ of these vector fields are circle diffeomorphisms, defined by setting $\sigma(0, \theta_2)$ to be the first point of intersection of the trajectory starting at $(0, \theta_2)$ with Σ . The dynamics of σ characterize the dynamics of the vector field up to topological equivalence. While many vector fields have the same return map, all of them are topologically equivalent. Moreover, the diffeomorphism σ can be *suspended* to create a vector field with σ as its return map [15]. A return map can also be defined to a cross-section of a principal foliation of a surface in $\mathcal{S}_{\mathcal{L}}$. Its trajectories will lie in intersections of lines of curvature with the cross-section. The dynamics of the return map will distinguish foliations with dense lines of curvature from foliations with closed lines of curvature.

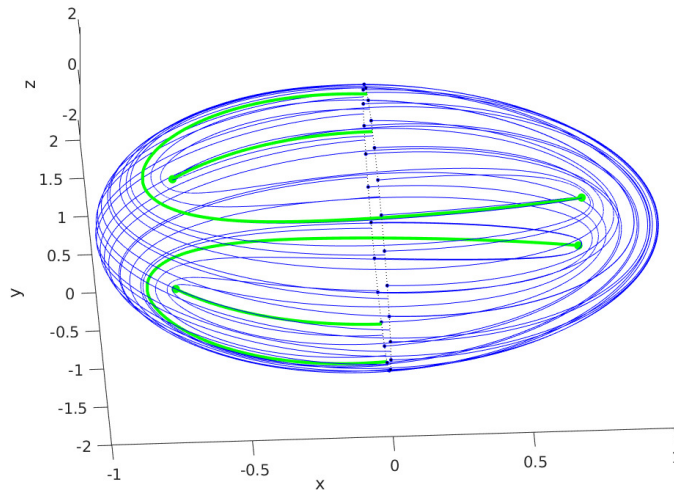


FIGURE 3. Lines of curvature that contribute to the definition of σ on the surface $S_{0.11}$. Σ is a light dotted black curve. Twenty-five points $w \in \Sigma$ are blue dots. Lines of curvature connecting the w with $\sigma(w)$ are blue curves. The four umbilic points are green dots and segments of their separatrices are heavy green curves.

Here is a construction of σ for surfaces $S \in \mathcal{S}_{\mathcal{L}}$ close to S_0 . The intersection Σ of S with the coordinate plane $x = 0$ is a global cross-section that divides S into two regions R_+ ($x > 0$) and R_- ($x < 0$). Define the map $\sigma : \Sigma \rightarrow \Sigma$ that follows lines of curvature into R_+ , then across Σ into R_- , and finally to the next intersection of that line of curvature with Σ . If $p \in \Sigma$, $\sigma(p)$ is the second point of intersection of the line of curvature starting at p with Σ . This definition fails on umbilic separatrices that approach an umbilic point before they return to Σ , but there is a continuous extension of σ to these points. Iterating σ gives successive intersections of lines of curvature with Σ in the direction from R_- to R_+ . Figure 3 visualizes the construction of σ for the surface $S_{0.11}$ and Figure 4 plots its graph on a mesh of one thousand points. The green vertical lines have values of $\theta \in \Sigma$ whose lines of curvature are umbilic separatrices which do not return to Σ .

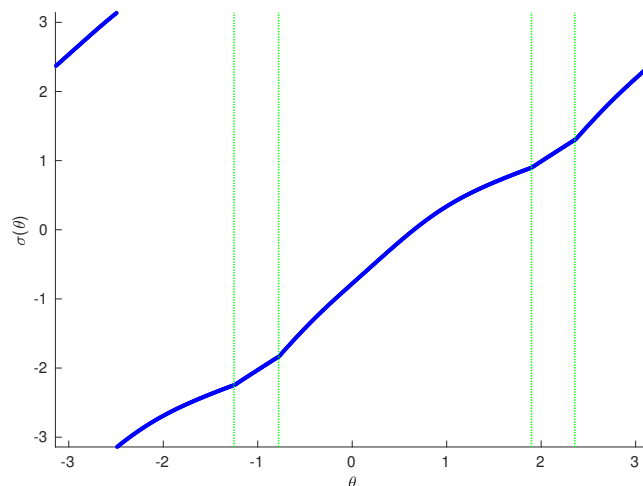


FIGURE 4. One thousand points on the graph of σ on the surface $S_{0.11}$. Σ is parameterized by an angular coordinate $\theta \in [-\pi, \pi]$. This graph represents a continuous curve on the torus, obtained by identifying $-\pi$ and π on both axes. The map $\sigma : \Sigma \rightarrow \Sigma$ is evidently a homeomorphism. The green vertical lines mark the location of intersections of separatrices with Σ .

For S_0 , the map σ is the identity (except at umbilic separatrices) since its lines of curvature are closed curves lying in the intersections of orthogonal quadric surfaces. Clearly σ_0 extends as the identity at intersections of umbilic separatrices with Σ : imagine the separatrix reaching the umbilic point and then retracing itself in the reversed direction. This paper analyzes σ near separatrices of lemon umbilic points on other surfaces S in $\mathcal{S}_{\mathcal{L}}$. The graph of σ in Figure 4 appears to have a *break* (jump in its first derivative) at the intersections of umbilic separatrices with Σ . Strong evidence for this observation is displayed in Figure 5 which shows finite difference approximations for the first and second derivatives of σ . The next section proves that the return maps of generic surfaces do have breaks at intersections with the separatrices of lemon umbilic points.

3. Breaks of Return Maps for Principal Foliations

This section analyzes breaks in the returns of principal foliations at separatrices of umbilic points. Figure 6 illustrates the geometry of these returns, using the surface $S_{0.02}$ defined by $x^2 + \frac{1}{3}y^2 + \frac{1}{5}z^2 + 0.02xyz = 1$ as an example. The figure shows a region around two umbilic points u_l and u_r to the left and right of the cross-section Σ defined by $x = 0$. Two lines of curvature straddling the black separatrix of u_l are plotted in blue and green from initial points $p_i, q_i \in \Sigma$ to their second intersections with Σ at p_f, q_f . These blue and green lines of curvature bend around the umbilic point in opposite directions. Decompose the return map σ as $\sigma_l \circ \sigma_r$ where $\sigma_r : \Sigma \rightarrow \Sigma$ is the first return map to Σ for lines of curvature entering

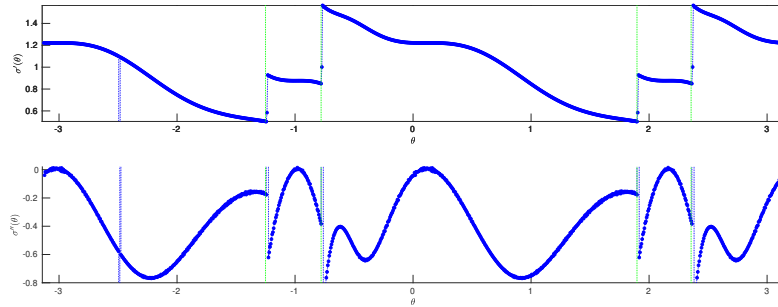


FIGURE 5. Finite difference approximations of the first and second derivatives σ' and σ'' of σ . These are computed by applying the matlab command `diff` to the vector of values of σ and then rescaling by the length of the mesh intervals of θ . The green vertical lines again mark the location of umbilic separatrix intersections with Σ

$R_+ = \{x > 0\}$ and σ_l is the first return map to Σ for lines of curvature entering $R_+ = \{x > 0\}$. The map σ_l above the intersection w of the separatrix with Σ is the inverse of σ_l below w since they connect the ends of the same lines of curvature in opposite directions. Thus, the limits of $\sigma'_l(u)$ as u approaches w from above and below are reciprocals. Since σ_l reverses orientation, they are different if the limit value is not -1 . Now observe that σ_r is smooth at w , so the limit values of σ'_l at w determine whether σ has a break at w . Figure 5 exhibits numerical evidence that there are breaks in the return map of $S_{0.11}$.

If the surface S does not have a break at the separatrix of a lemon, I assert that there are perturbations of S which do have breaks at this separatrix. A precise statement is the following theorem:

Theorem 3.1. *Let S be a surface with a lemon umbilic point and Σ a cross-section intersecting its separatrix transversally at the point p . If the return map $\sigma : \Sigma \rightarrow \Sigma$ does not have a break at p , there are perturbations of S that do.*

Proof. The crux of the proof of this theorem is to calculate the breaks of a prototypical family analytically. It will be apparent that the construction of this family can be modified to perturb surfaces without a break at a lemon separatrix to ones that do have a break.

Monge coordinates for a surface S represent the surface as the graph of a function $g : \mathbb{R}^2 \rightarrow \mathbb{R}$ with $g(0) = dg(0) = 0$. The origin is an umbilic point of the Monge surface if and only if d^2g is a multiple of the identity. Whether this umbilic point is generic and its type is determined by the cubic terms in the Taylor expansion of g [16, 2]. Monge coordinates can be introduced at any point of a surface by an orthonormal transformation around that point. Thus, there is no loss of generality in analyzing breaks by restricting attention to surfaces in Monge form near an umbilic point.

Consider the family of surfaces M_a defined implicitly by $w - (u^2 + v^2 - 8u^3 - 8uv^2 + av^3) = 0 = g_a(u, v, w)$ with small parameter a . The origin is a lemon umbilic

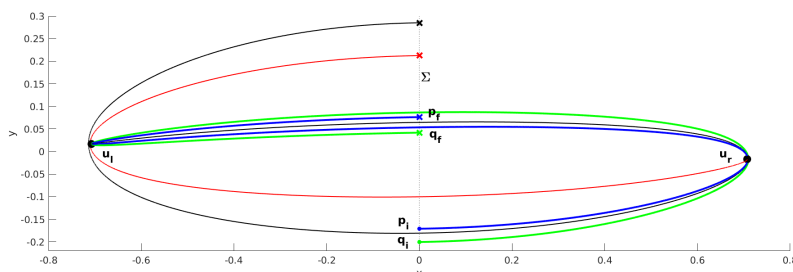


FIGURE 6. Two umbilic points on $S_{0.02}$ and segments of their separatrices, plotted in black and red. Segments of two additional lines of curvature with initial points p_i and q_i on the cross-section Σ are plotted as blue and green curves. The images p_f and q_f of these points under σ are marked by x's. The blue and green initial points straddle the intersection of the black separatrix with Σ . The blue line of curvature starts at p_i above the black separatrix, stays to the left of the separatrix as it bends around the right umbilic point u_r , and then bends around the left umbilic point u_l to intersect Σ above the black separatrix at p_f . The green line of curvature does the opposite: it starts below the black separatrix at q_i , stays to the right of the separatrix as it bends around the right umbilic point, and then bends around the left umbilic point to intersect Σ below the black separatrix at q_f . The points p_i and q_i can be chosen so that the segments of their lines of curvature to the left of Σ coincide, but with opposite orientations.

point of all the M_a . When $a = 0$, g is even in y and M_0 is symmetric with respect to the reflection $v \rightarrow -v$. Consequently, the separatrix lies along the u axis and the return map σ_0 of the cross-section $u = -0.1$ is $\sigma_0(v) = -v$. As a varies from 0, the separatrix of the origin remains along the u axis, but the return map σ_a changes as described below.

The normal vector N to M_a is parallel to $dg = (-g_u, -g_v, g_z)$. Principal vectors of M_a satisfy the Rodrigues formula $\det(N, \xi, dN \cdot \xi) = 0$ or equivalently $\det(dg, \xi, d^2g \cdot \xi) = 0$. Writing the vector ξ as (x, y, z) , the modified Rodrigues formula is a polynomial equation in (u, v, w, x, y, z) . Eliminating w, z from this equation by solving $g = 0$ for w and $dg \cdot \xi = 0$ for z leaves an equation $\bar{R}(u, v, x, y) = 0$ that is homogeneous quadratic in (x, y) . Solutions of $\bar{R} = 0$ give projections $(x(u, v), y(u, v))$ of the principal directions of M_a to the tangent space of the (u, v) plane. Although the principal foliation is not orientable, off the u axis it contains a vector field normalized so that $x = \dot{u} = 1$. Integrating the normalized vector fields $X_a = (1, y_a(u, v))$ produces projections of the lines of curvature to the (u, v) plane. The goal here is to prove that as a varies y_a is a monotonic function of a , so that the vector fields X_a are transverse to each other.

The function $y_a(u, v)$ is obtained by solving $\bar{R} = 0$ with $x = 1$. Since the algebraic expressions are moderately complicated, the Taylor series of $y_a(u, v) - y_0(u, v)$ as a function of v was computed from \bar{R} using the symbolic toolbox of Matlab. These

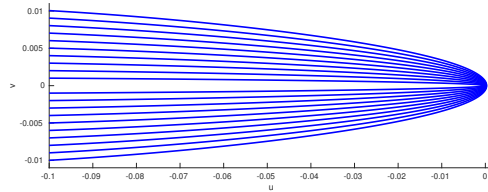


FIGURE 7. Ten lines of curvature of the Monge surface $M_{0.01}$ with initial values equally spaced in the interval $[-0.01, -0.001]$ on the line $u = -0.1$.

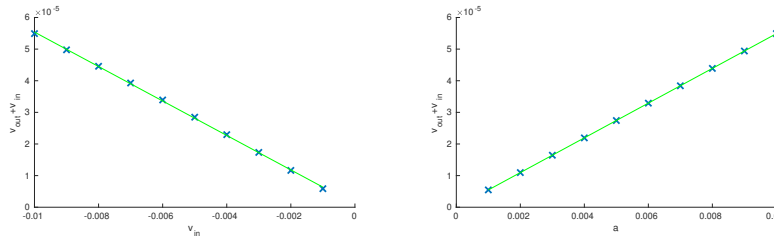


FIGURE 8. Deviation of the return map σ_a for the Monge surfaces M_a from $\sigma_0(v) = -v$. For the lines of curvature displayed in Figure 7, the left panel plots the quantity $\sigma_{0.01}(v) + v$ vs. the initial v . The green line is a linear fit to this data. The right panel of the figure plots values of $\sigma_a(-0.01) - 0.01$ for ten values of a in the interval $[0.001, 0.01]$.

calculations approximate $y_a(u, v) - y_0(u, v)$ as $-3av \frac{576 u^3 - 72 u^2 + 2 u}{-576 u^4 + 96 u^3 - 4 u^2 - 1} + o(av^2)$ which is negative when $a > 0$ and $v > 0$ are small and $u \in [-0.1, 0)$. This implies that $y_a(u, v)/(av)$ is bounded away from 0 in rectangles $[-0.1, -u_0] \times [-v_0, v_0]$ for $u_0 > 0$ and $v_0 > 0$ sufficiently small. Integration over lines of curvature of M_a demonstrates that the return map of M_a has a break at $v = 0$ with jump of its derivative comparable to a . Figure 7 displays lines of curvature for the surface $M_{0.01}$, showing how they bend around the umbilic point at the origin. Figure 8 illustrates the fit of return maps of the M_a to the estimates derived above. The left panel fixes $a = 0.01$ and plots the dependence of $\sigma_{0.01}(v) + v$ on v . The right panel fixes $v = -0.01$ and plots $\sigma_a(v) - 0.01$ as a function of a . Linear fits to these data are very good indeed. These calculations establish that return maps of the surfaces M_a , $a \neq 0$ have breaks at the separatrix of the origin, which is the u axis.

Summarizing, the surface S_0 whose return map is smooth at the separatrix of a lemon umbilic point p is embedded in a family of surfaces S_a so that p and its separatrix remain fixed as a varies, but the derivative of the return map at the separatrix changes at a non-zero rate as a varies. The calculations are algebraic, so in the space of surfaces in Monge form that have a lemon umbilic point at the origin, those which do not have a break in their return map will be an algebraic

variety. Since algebraic varieties are closed sets of lower dimension than the space in which they sit, there is a dense, open subset of surfaces with a lemon umbilic point whose return maps have a break at the separatrix of the umbilic point.

□

4. Homeomorphisms of the Circle with Breaks

Homeomorphisms of the circle S^1 are a remarkable class of dynamical systems that has been studied extensively, beginning with Poincaré in the nineteenth century. Herman [7] and de Melo and van Strien [4] gave systematic presentations that preceded the definitive results of Yoccoz [18] cited in the award of his 1994 Fields medal. Since my analysis of principal foliations for surfaces in $\mathcal{S}_{\mathcal{L}}$ is based upon this theory, I recall relevant results. This section parameterizes the circle S^1 as \mathbb{R}/\mathbb{Z} and sets $\pi : \mathbb{R} \rightarrow S^1$ to be the projection.

If $f : S^1 \rightarrow S^1$, *lifts* of f are maps $F : \mathbb{R} \rightarrow \mathbb{R}$ that satisfy $\pi \circ F = f \circ \pi$. Since $\pi(x + 1) = \pi(x)$, $F(x + 1) = F(x) + 1$. This identity establishes a close connection between orientation preserving circle homeomorphisms and increasing maps of \mathbb{R} that commute with the translation $T(x + 1) = x + 1$. If F is a lift of the homeomorphism f , the *rotation number* $\rho(F)$ of F is

$$\lim_{n \rightarrow \infty} \frac{F^n(x) - x}{n}.$$

The rotation number $\rho(F)$ is independent of $x \in \mathbb{R}$, and $\rho(F) \pmod{1}$, regarded as a point on the circle, is the rotation number $\rho(f)$ of f .

Geometrically, a homeomorphism $f : S^1 \rightarrow S^1$ preserves the cyclic order of points on the circle: if $\theta_1 < \theta_2 < \theta_3$, then $f(\theta_1) < f(\theta_2) < f(\theta_3)$. Consequently, if θ is periodic of period n , then the points $f^j(\theta)$, $0 \leq j < n$, partition S^1 into n intervals that are permuted by f , and f^n maps each of these intervals onto itself by an increasing function. A corollary of this observation is that all trajectories will tend to a periodic orbit of period n . It is immediate that $n\rho(f) = 0$. On the other hand, there are homeomorphisms without periodic orbits: the translations $T_\omega(x) = x + \omega$ with ω irrational are fundamental examples. Note that $\rho(T_\omega) = \omega$. If f is a homeomorphism with irrational $\rho(f) = \omega$, the cyclic order of points in its trajectories agree with those of $\pi \circ T_\omega$. A basic theorem of Poincaré is that a homeomorphism $f : S^1 \rightarrow S^1$ has periodic orbits if and only if $\rho(f)$ is rational. The Denjoy Theorem states that if $f : S^1 \rightarrow S^1$ is C^1 , its derivative has bounded variation and $\rho(f) = \omega$ is irrational, then all of the trajectories of f are dense in S^1 .

If f_λ is a smooth family of diffeomorphisms and $\frac{\partial F}{\partial \lambda} > 0$, then $\frac{\partial \rho(F)}{\partial \lambda} \geq 0$. In generic families, the graph of $\rho(f)$ vs λ is a “devil’s staircase.” Specifically, it assumes each rational value on a closed interval and each irrational value at a single point. For smooth families of diffeomorphisms, more is known. If f_λ is $C^{3+\epsilon}$, then the set of λ with ρ irrational has positive Lebesgue measure even though it is nowhere dense. I explain more about this result since the return maps constructed from principal foliations seem to have different behavior.

Let f_λ be a $C^{3+\epsilon}$ family of circle diffeomorphisms with lifts F_λ . When f_λ has irrational rotation number ω , Denjoy’s theorem implies that its trajectories are all dense. Since the trajectories of f have the same cyclic order as those of the rotation

$R_\omega = \pi \circ T_\omega$, the map h that sends $f^n(0)$ to $n\omega \pmod{1}$ extends to a topological conjugacy of f with R_ω : $h \circ f = R_\omega \circ h$. The only topological conjugacies of an irrational rotation with itself are rotations, so the conjugacy h is unique up to a composition with a rotation. Remarkably, if ω satisfies a *Diophantine condition*, then the conjugacy h is smooth [18]. Since smooth maps are almost linear on short length scales, the relative distances between adjacent points in a long finite trajectory $f^j(x)$, $0 < j < N$ approximate those of the rotation R_ω . Moreover, the derivative of f^j is uniformly bounded, with a bound independent of j because $f^j = h^{-1} \circ R_{j\omega} \circ h$ and $(R_{j\omega})' \equiv 1$.

Periodic orbits of f with rotation number p/q are projected solutions of the equation $F_\lambda^q(x) = x + p$. In generic families, the solutions of this equation constitute a smooth curve in the (x, λ) plane, invariant under the translation $(x, \lambda) \rightarrow (x + 1, \lambda)$. The range of λ on this curve is the width of the step at value p/q for the devil's staircase function $\rho(F_\lambda)$. In order for the parameter set with $\rho(F_\lambda)$ irrational to have positive measure, the widths of the phase locked steps with $\rho(F_\lambda) = p/q$ must decrease rapidly with q . If F_λ is the translation $T(x) = x + \omega$, then $T^q(x) = x + q\omega$ for all x and the phase locked step shrinks to a single point. In other families, $\frac{\partial}{\partial \lambda}(F^q(x) - x)$ grows linearly with q and the derivative of $F^q(x) - x$ decreases rapidly with q . The speed of the decrease is closely related to the results about smooth conjugacy described above. Renormalization is a strategy for analyzing both the smoothness of conjugacies and the widths of phase locked steps.

The ordering of trajectories of a homeomorphism $f : S^1 \rightarrow S^1$ with rotation number ω can be inferred from the expression of ω as a continued fraction or, equivalently, its trajectory under the Gauss map $\omega \rightarrow 1/\omega \pmod{1}$. Iterates $f^n(x)$ which are closer to x than previous iterates $f^j(x)$, $0 < j < n$, are of particular interest. Two concepts facilitate the study of these closest returns:

- If J is a subinterval of the circle, then the *induced map* $\hat{f} : J \rightarrow J$ is defined by $\hat{f}(x) = f^j(x)$ with $j > 0$ the smallest positive integer for which $f^j(x) \in J$. Note that \hat{f} is usually discontinuous at points where $\hat{f}(x)$ is in the boundary of J .
- *Renormalization* combines the construction of an induced map with rescaling the length of J to a standard size (usually 1).

Renormalization can be viewed as an operator on the space of circle homeomorphisms without fixed points. Since the trajectories of maps with irrational rotation number ω have the same order as those of the rotation R_ω , it suffices to describe successive renormalizations for R_ω . The trajectory of 0 for the rotation $R_\omega(x) = x + \omega$ consists of the points $n\omega \pmod{1}$. The point $x_l = q_l\omega \pmod{1}$ is a left nearest neighbor of $0 \in S^1$ if $x^n \in (x_l, 0)$ implies $n > q_l$. Similarly, $x_r = q_r\omega \pmod{1}$ is a right nearest neighbor of 0 if $x^n \in (0, x_r)$ implies $n > q_r$. Assume further that $x_l + x_r < 0$ if $q_r > q_l$ and $x_l + x_r > 0$ if $q_r < q_l$. The induced map \hat{R}_ω of R_ω on the interval $[x_l, x_r]$ then has two branches: $R_\omega^{q_r} : [x_l, 0] \rightarrow [f^{q_r + q_l}(0), x_r]$ and $R_\omega^{q_l} : [0, x_r] \rightarrow [x_l, f^{q_r + q_l}(0)]$. Identifying x_l with x_r and rescaling \hat{R}_ω by a factor of $x_r - x_l$ produces a new homeomorphism of S^1 .

If $x_l < 0 < x_r$ are nearest neighbors of 0 with $x_r + x_l > 0$, then the smallest right nearest neighbor x_r^* of 0 with $q_r^* > q_l$ has $q_r^* = q_r + kq_l$ where k is the integer with $q_r + (k + 1)q_l < 0 < q_r + kq_l$. Equivalently, k is the integer part of $-x_r/x_l$. It also is a term in the continued fraction expansion of ω . With rescaling, the

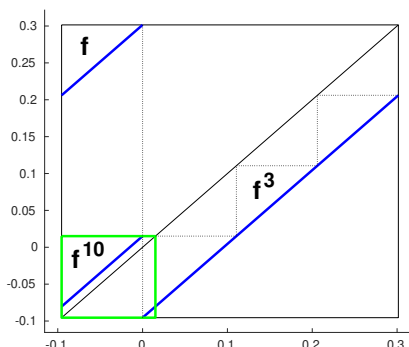


FIGURE 9. An induced map of the rotation $f(x) = x + \frac{1}{\sqrt{11}} \pmod{1}$. Initially, f was replaced by f^3 in the interval $[0, f(0)]$, producing the discontinuous map enclosed in the black square. The next induced map replaces f by f^{10} in the interval $[f^3(0), 0]$, producing the map on $[f^3(0), f^{10}(0)]$ with branches f^{10} and f^3 displayed in the green square.

renormalization operator \mathcal{R} maps the induced map on $[x_l, x_r]$ to the induced map on $[x_l, x_r^*]$. Its iterates are rescaled induced maps on intervals joining left and right nearest neighbors in the trajectory of 0.

Figure 9 displays the first two induced maps for the rotation $f(x) = x + \frac{1}{\sqrt{11}}$. The points in $[f^3(0), 0]$ are mapped by f itself into $[f^4(0), f(0)]$, while f^3 maps $[0, f(0)]$ to $[f^3(0), f^4(0)]$. The black square encloses this map which was induced from f to the interval $J = [f^3(0), f(0)]$. The next induced map has domain $[f^3(0), f^{10}(0)]$ and branches f^{10} on $[f^3(0), 0]$ and f^3 on $[0, f^{10}(0)]$. Its values at both endpoints of J are $f^{13}(0)$.

For a general circle diffeomorphism f , renormalization replaces f by iterates that are closest returns. A key observation is that if the rotation number of f satisfies a Diophantine condition, the trajectories of the renormalization operator converge to maps whose branches are translations. This observation is based upon analysis of *distortion* of the maps. A scale invariant measure of the “nonlinearity” of an increasing map $f : J \rightarrow J$ is the maximum value of $\log(\frac{f'(y)}{f'(x)}) = \log(f'(y)) - \log(f'(x))$ for $x, y \in J$. The distortion of rotations is zero, so the iterates of a map smoothly conjugate to a rotation have bounded distortion. The converse is also true [7]. Now, the fundamental theorem of calculus gives

$$\log(f'(y)) - \log(f'(x)) = \int_x^y \frac{f''(u)}{f'(u)} du$$

and the chain rule implies

$$\log((f^n)'(y)) - \log((f^n)'(x)) = \sum_{j=0}^{n-1} \log(f'(f^j(y))) - \log(f'(f^j(x))).$$

Thus, bounds on f''/f' and the sum of the lengths of the first n iterates of J give bounds on the distortion of f^n on J . If n is an iterate appearing in the renormalizations of f and $J = [x, f^n(x)]$, the intervals $f^j(J)$, $0 \leq j < n$ are disjoint, establishing a uniform bound on the distortion of f^n on J .

In addition to the quantity f''/f' as an infinitesimal measure of nonlinear distortion, the *Schwarzian derivative* $S(f) = \frac{f'''}{f'} - \frac{3}{2}\left(\frac{f''}{f'}\right)^2$ is an infinitesimal measure of how much f deviates from a fractional linear transformation $\phi(x) = \frac{ax+b}{cx+d}$. Straightforward calculations yield the composition formula $S(g \circ f)(x) = (S(g))(f(x))(f'(x))^2 + S(f(x))$ and the result that Sf is identically 0 if and only if f is a fractional linear transformation. Estimates of the Schwarzian derivative of iterates of a circle diffeomorphism lead to stronger estimates of their distortion. The Schwarzian derivative of f^n is a sum of n terms which are individually bounded while renormalization rescales f^n by a factor comparable to n , so the Schwarzian derivative of the renormalized f is comparable to $1/n$. This suggests that the sequences of renormalizations of f converge locally to fractional linear transformations. In the case of diffeomorphisms, boundary conditions on the renormalizations imply that the only fractional linear transformations that can be limits are rotations. On the other hand, if f has breaks (jump discontinuities of its derivative), then the iterates of f do as well. Moreover, in a finite trajectory of length n that has a single break, the ratio of the left and right derivatives of f^n is the same as that of f at the break. Thus the limits of renormalization in a map f with a finite number of breaks are piecewise fractional linear transformations, joined at breaks with derivative ratios determined by those of f itself. This observation is largely responsible for the result of Khanin and Vul [10] that periodic orbits occur at a full measure set of parameters in generic families of diffeomorphisms with a single break whose derivative jump has magnitude bounded away from one.

Turn now to families of lifts of homeomorphisms $f_\lambda : S^1 \rightarrow S^1$ in which $f_\lambda(x)$ is a strictly increasing function of λ and the range of the rotation number function $\rho(f_\lambda)$ is $[0, 1]$. Iterates of f are readily seen to also be increasing functions of λ . Maps with rational rotation number p/q have lifts F that are solutions of the equation $F_\lambda^q(x) = x + p$. For fixed x , this equation can only have a single solution because $F_\lambda^q(x)$ increases with λ . Since the range of the rotation number function includes p/q in its interior then there will be a solution of $F_\lambda^q(x) = x + p$ for every x . Consequently, unless $F_\lambda^q(x) - x - p$ is identically zero for a fixed λ , there will be an interval $\Lambda_{p/q}$ of λ values with solutions of $F_\lambda^q(x) = x + p$. Mimicking the construction of Cantor sets as a nested intersection of sets C_n consisting of 2^n disjoint intervals can determine whether the union of the $\Lambda_{p/q}$ has full Lebesgue measure and the set of λ with irrational rotation numbers has zero measure.

The *Farey tree* of rational numbers relates the pattern of renormalizations of a map to its rotation number. Beginning with 0 and 1, the Farey tree of rational numbers is constructed inductively in levels. Each pair of adjacent nodes $p/q < p'/q'$ at level n has child $(p+p')/(q+q')$ which is inserted as a level $n+1$ node. The difference $p'/q' - p/q = 1/qq'$ of adjacent numbers in the Farey tree is as small as possible for rational numbers with these denominators. If p/q is in level n of the Farey tree and its two children in level $n+1$ are p_l/q_l and p_r/q_r , homeomorphisms with rotation number $p_l/q_l < \rho < p_r/q_r$ use the same iterates in their successive renormalizations to this level. Restricting a family of homeomorphisms f_λ to the

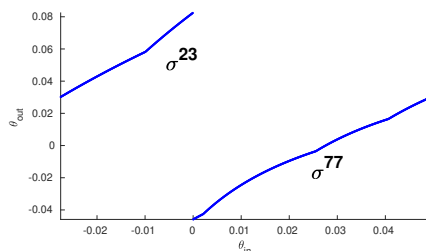


FIGURE 10. A renormalization of the return map of the surface $S_{0.11}$ to an interval bounded by a pair of nearest neighbors to the trajectory of $\theta = 0$.

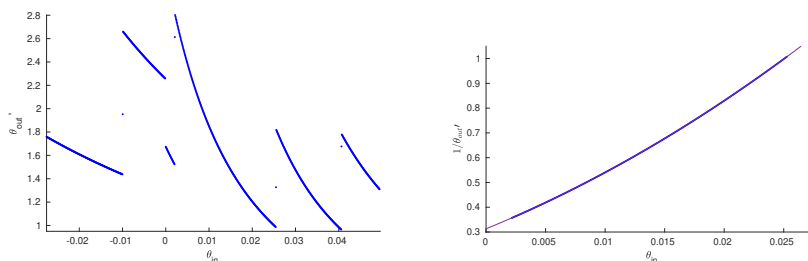


FIGURE 11. The left graph plots finite difference calculations of the derivative of the renormalized return map shown in Figure 10. The right graph compares the renormalized return map $\hat{\sigma}$ with a fractional linear transformation by fitting a parabola to $1/(\hat{\sigma}')^2$

subfamily with rotation numbers in the interval $(p_l/q_l, p_r/q_r)$ produces a family in which the period orbits of f with rotation number p/q become fixed points of the n th renormalization \hat{f}_λ . Additionally, the rotation numbers of the renormalized family \hat{f}_λ cover the full interval $(0, 1)$. If q is large, estimates of distortion and Schwarzian derivatives imply that the \hat{f}_λ have bounded distortion and are approximately fractional linear transformations.

Figure 10 displays a renormalization $\hat{\sigma}$ (without rescaling) of the return map σ of $S_{0.11}$, shown in Figure 4. The two branches of $\hat{\sigma}$ are σ^{23} and σ^{77} . Figure 11 plots estimates of the derivative of $\hat{\sigma}$. The breaks of σ persist in $\hat{\sigma}$, and the derivative increases across each jump. The discontinuity at $\theta = 0$ results from the change of branches rather than a jump of the derivative. The derivative of a fractional linear transformation $\frac{ax+b}{cx+d}$ is $(ad - bc)/(cx + d)^2$, so its reciprocal is a quadratic polynomial. Figure 11 also tests how closely the fourth branch of $\hat{\sigma}$ approximates a fractional linear transformations by computing $1/(\hat{\sigma}')^2$ and overlaying a parabola. The fit is striking.

I return now to the question: does the parameter set C with dense lines of curvature in a family of surfaces S_λ have zero measure? Denote by C_n the closure of the parameter set of λ that do not have closed lines of curvature represented by

periodic orbits of the return map with Farey level at most n . As in the construction of the classical Cantor set, C_{n+1} is obtained by removing an open interval from each component of C_n , and C is the nested intersection of the C_n . Denote one dimensional Lebesgue measure by μ . If the relative length of the interval removed from each component is always bounded below by $0 < \beta < 1$, then $\mu(C_n) < (1 - \beta)^n \mu(C_0)$. This implies C has measure zero, a conclusion that continues to hold with the weaker property that the bound on relative lengths holds infinitely often in every sequence of nested intervals whose intersection is a point of C . Thus, the key issue is to obtain bounds on

$$\frac{\mu(\rho^{-1}(p/q))}{\mu(\rho^{-1}(p_l/q_l, p_r/q_r))} \quad (4.1)$$

where p_l/q_l and p_r/q_r are Farey neighbors of p/q and $\rho(\lambda)$ is the rotation number of the return map of the surface S_λ .

Khanin and Vul [10] found the desired bound on relative lengths (4.1) in families of circle diffeomorphisms with a single break whose derivative jumps all have magnitude at least $\alpha > 1$. Renormalization preserves such families and successive renormalizations tend to families of piecewise fractional linear transformations ϕ with a single break of magnitude at least α . If the break is translated to the origin in the domain and range, ϕ will have the form $\phi(x) = ax/(1 + (a - 1)x)$ since $\phi(0) = 0$ and $\phi(1) = 1$. The magnitude of the break is $\phi'(0)/\phi'(1) = a^2$. Moreover, if $a > 1$ the range of $\phi(x) - x$ is $[0, \sqrt{a} - 1/\sqrt{a}]$. This leads to a lower bound on the quantity (4.1) and the conclusion that the set of parameters with irrational rotation number has measure zero.

Khmelev [11] discussed the extension of the results to Khanin and Vul [10] to families with multiple breaks, but characterization of which families have phase locked parameter sets of full measure remains an open question. In families where the product of break sizes in each trajectory with breaks is one, the breaks can disappear in induced maps whose branches encompass all of the breaks in individual trajectories. This cancellation cannot occur if all of the breaks have derivative jumps in which the derivative increases. Figure 5 shows that this is indeed the case for the surface $S_{0.11}$. So we impose the additional constraint on the space of surfaces $\mathcal{S}_{\mathcal{L}}$ that that derivatives increase across jumps.

The return maps of surfaces in the class $\mathcal{S}_{\mathcal{L}}$ have four umbilic points, each lemons. The previous section establishes that generic surfaces have return maps with breaks at intersections of a cross-section with umbilic separatrices. The numerical calculation of the return map of the surface $S_{0.11}$ displayed in Figures 4 and 5 show these breaks. At each break, the derivative jumps up. Since the cumulative derivative jump in a trajectory with multiple breaks is the product of the individual jumps, renormalizations of these return maps have breaks of at least the same magnitude as the original return map. Moreover, it appears that σ'' is almost negative. This prompts consideration of families of circle homeomorphisms consisting of piecewise, concave down linear fractional transformations with k breaks, at each of which the derivative increases.

Theorem 4.1. *Assume $\sigma_\lambda : S^1 \rightarrow S^1$, $\lambda \in \Lambda$ is a family of homeomorphisms such that*

- σ_λ is a piecewise fractional linear transformation on each of the intervals in the partition with boundary points $[x_1, x_2, \dots, x_k, x_1]$. The x_j may depend on λ .
- $\sigma''_\lambda < 0$
- The left and right derivatives $h'_{\lambda-}(x_j) = a_j$, $h'_{\lambda+}(x_j) = b_j$ satisfy $a_j > 0$, $b_j > 0$ and $b_j/a_j > \alpha > 1$
- The rotation number function $\rho : \Lambda \rightarrow S^1$ that assigns the rotation number of σ_λ to λ is onto.

Then $\rho^{-1}(\mathbb{R} - \mathbb{Q}) \subset \Lambda$ has measure zero.

Proof. Each phase locked interval $\rho^{-1}(p/q)$ is contained inside $\rho^{-1}(p_l/q_l, p_r/q_r)$ where $(p_l/q_l, p_r/q_r)$ is the Farey interval of p/q . To prove the theorem, it suffices to establish the estimate (4.1) holds for each p/q . The renormalization operator maps the space of fractional linear transformations satisfying the hypotheses of the theorem to itself, except that the partition size k may decrease if there is a trajectory containing multiple partition points. This reduces the estimate (4.1) for rotation number p/q to that for rotation number 0.

The function σ'_λ decreases on each partition interval I_j . Let $c > 1$ be a lower bound for $\sigma'_\lambda(x_j)/\sigma'_\lambda(x_{j+1})$, quantifying the derivative drop across I_j . Since σ'_λ is a decreasing function on each I_j , c also is a lower bound for the derivative drop across branches of its renormalizations \hat{h}_λ . Let $J_j = [u_j, u_{j+1}]$ be a partition interval of the renormalization \hat{h} with length $u_{j+1} - u_j \geq 1/k$ and assume that the range of $\hat{h}(x) - x$ has length smaller than δ . If $v_0 = \hat{h}(u_j) - u_j$, $v_1 = \hat{h}((u_j + u_{j+1})/2) - (u_j + u_{j+1})/2 - v_0 + d_1$ and $v_2 = \hat{h}(u_{j+1}) - u_{j+1} - v_0 + d_2$ with $d_1 < \delta$, $d_2 < \delta$, then there is a unique fractional linear transformation that interpolates the points (u_j, v_0) , $((u_j + u_{j+1})/2, v_1)$, (u_{j+1}, v_2) . Explicit computation yields $\hat{h}'(u_j) = 1 - (4d_1 + d_2)/(u_{j+1} - u_j) + o(\delta)$ and $\hat{h}'(u_{j+1}) = 1 + (4d_1 + 3d_2)/(u_{j+1} - u_j) + o(\delta)$. This implies that $\hat{h}'(u_j)/\hat{h}'(u_{j+1}) > 1 + 12k\delta + o(\delta)$ so that δ has a lower bound comparable to $(c - 1)/12k$, independent of the renormalization. This estimate completes the proof of the theorem. \square

Together with the numerical computation of the surfaces defined by (2.2), Theorem 4.1 locates an open region \mathcal{U} in the space of C^r , $r > 3$, surfaces inside which closed lines of curvature are *prevalent* [9]; i.e., in generic one parameter families, parameter sets yielding surfaces with dense lines of curvature have measure zero. This dynamical behavior stands in contrast to that of families of vector fields on the torus T^2 , where quasiperiodic dynamics occurs at positive measure sets of parameters. It remains an open question whether there are regions in the space of simply connected surfaces where closed lines of curvature are not prevalent. Even in the finite dimensional space of piecewise fractional linear transformations of S^1 with multiple breakpoints, it is not known whether those with dense trajectories constitute a set of measure zero. Finally, I note that there are surfaces that have both global cross-sections and more than four umbilic points. Their return maps are *generalized interval exchange maps* [12] of S^1 with discontinuities and still more complicated dynamics than circle diffeomorphisms with breaks. Further study of these one dimensional maps can give additional insight into the geometry of principal foliations of embedded surfaces.

References

- [1] M V Berry and J H Hannay. Umbilic points on gaussian random surfaces. *Journal of Physics A: Mathematical and General*, 10(11):1809–1821, nov 1977.
- [2] J. W. Bruce and D. L. Fidal. On binary differential equations and umbilics. *Proc. Roy. Soc. Edinburgh Sect. A*, 111(1-2):147–168, 1989.
- [3] Gaston Darboux. *Leçons sur la théorie générale des surfaces et les applications géométriques du calcul infinitésimal*, 1887.
- [4] Wellington de Melo and Sebastian van Strien. *One-dimensional dynamics*, volume 25 of *Ergebnisse der Mathematik und ihrer Grenzgebiete (3) [Results in Mathematics and Related Areas (3)]*. Springer-Verlag, Berlin, 1993.
- [5] Ronaldo Garcia and Jorge Sotomayor. *Differential equations of classical geometry, a qualitative theory*. Publicações Matemáticas do IMPA. [IMPA Mathematical Publications]. Instituto Nacional de Matemática Pura e Aplicada (IMPA), Rio de Janeiro, 2009. 27o Colóquio Brasileiro de Matemática. [27th Brazilian Mathematics Colloquium].
- [6] John Guckenheimer. Dense lines of curvature on convex surfaces. *Proc. Amer. Math. Soc.*, 148(8):3537–3549, 2020.
- [7] Michael-Robert Herman. Sur la conjugaison différentiable des difféomorphismes du cercle à des rotations. *Inst. Hautes Études Sci. Publ. Math.*, (49):5–233, 1979.
- [8] Morris W. Hirsch, Stephen Smale, and Robert L. Devaney. *Differential equations, dynamical systems, and an introduction to chaos*. Elsevier/Academic Press, Amsterdam, third edition, 2013.
- [9] Brian R. Hunt, Tim Sauer, and James A. Yorke. Prevalence: a translation-invariant “almost every” on infinite-dimensional spaces. *Bull. Amer. Math. Soc. (N.S.)*, 27(2):217–238, 1992.
- [10] K. M. Khanin and E. B. Vul. Circle homeomorphisms with weak discontinuities. In *Dynamical systems and statistical mechanics (Moscow, 1991)*, volume 3 of *Adv. Soviet Math.*, pages 57–98. Amer. Math. Soc., Providence, RI, 1991. Translated from the Russian by V. Nazaïkinskiĭ.
- [11] D. V. Khmelev. Rational rotation numbers for homeomorphisms with several break-type singularities. *Ergodic Theory Dynam. Systems*, 25(2):553–592, 2005.
- [12] Stefano Marmi, Pierre Moussa, and Jean-Christophe Yoccoz. Linearization of generalized interval exchange maps. *Ann. of Math. (2)*, 176(3):1583–1646, 2012.
- [13] Gaspard Monge. Sur les lignes de courbure de la surface de l’ellipsoïde. In *Application de l’Analyse à la Géométrie (5th edition)*, pages 139–160. Bachelier, Paris, 1796.
- [14] M. M. Peixoto. Structural stability on two-dimensional manifolds. *Topology*, 1:101–120, 1962.
- [15] S. Smale. Differentiable dynamical systems. *Bull. Amer. Math. Soc.*, 73:747–817, 1967.
- [16] J. Sotomayor and C. Gutiérrez. Structurally stable configurations of lines of principal curvature. In *Bifurcation, ergodic theory and applications (Dijon, 1981)*, volume 98 of *Astérisque*, pages 195–215. Soc. Math. France, Paris, 1982.

- [17] Jorge Sotomayor and Carlos Gutiérrez. *Structurally stable configurations of lines of curvature and umbilic points on surfaces*, volume 3 of *Monografías del Instituto de Matemática y Ciencias Afines [Monographs of the Institute of Mathematics and Related Sciences]*. Instituto de Matemática y Ciencias Afines, IMCA, Lima; Universidad Nacional de Ingeniería, Instituto de Matemáticas Puras y Aplicadas, Lima, 1998.
- [18] J.-C. Yoccoz. Conjugaison différentiable des difféomorphismes du cercle dont le nombre de rotation vérifie une condition diophantienne. *Ann. Sci. École Norm. Sup. (4)*, 17(3):333–359, 1984.

John Guckenheimer
Mathematics Department,
Cornell University,
Ithaca, NY 14850
USA
jmg16@cornell.edu